

Prediction of cavitation erosion occurring in a control valve using computational fluid dynamics (CFD)

Kenji Saito^{1, *}, Youn Chongho¹

¹Department of valve product development, Azbil Corporation, Kanagawa, Japan

*corresponding author: k.saito.ht@azbil.com

Abstract Control valves are used to control the flow of fluid through piping systems in plants and factories. If the fluid is a liquid, cavitation may occur due to vortices or increase in local flow velocity. In this study, we visualize and validate the cavitation flow using computational fluid dynamics (CFD). A 1.5" valve with a flow-to-open direction was used to compare the experimental results with those of Yuzawa et al. A homogeneous flow model was used to represent a cavitation flow, and a turbulent calculation model using large-eddy simulation was used to express the state of the vortex directly. The visual result of the CFD modelling of cavitation flows showed that the appearance of cavitation is similar to experimental results and agrees well with the flow coefficient C_v . Cavitation modelling was also used to evaluate erosion indexes under an upstream pressure $P_U = 20$ MPa and cavitation coefficient $\sigma = 1.005$. The results prove that the erosion index is effective for the prediction of the points where the cavitation erosion occurs.

Keywords: control valve, erosion, CFD, cavitation

1 Introduction

Control valves are used to control the flow of fluid through piping systems in a variety of plants and factories. They are required to operate reliably for a long time and must guarantee accurate flow characteristics. These requirements need to be fulfilled for all types of fluids.

The degree to which the valve is open is controlled by the control valve and if the fluid is a liquid, cavitation may occur due to vortices or increase in local flow velocity. Cavitation is a phenomenon in which bubbles are formed when the pressure of the liquid drops below the saturated vapor pressure. When the pressure rises above the saturated steam pressure again, the bubbles collapse and eject high pressure micro jets. A collapsing bubble in close proximity will exert high stress to the pipe wall and cause erosion.

Cavitation erosion occurs in various fluid machines such as pumps and ship propellers. It often occurs near the plug of a control valve resulting in flow deterioration, difficulties in shutting off the valve and can even lead to plant shutdown.

Cavitation erosion research has therefore been conducted for a long time. Kuiper visualized the generation of vortex cavitation occurring in ship propellers, and proposed a blade shape with a low risk of cavitation erosion [1] while Yuzawa visualized cavitation erosion in control valves caused by high-pressure angle valve [2]. Other studies have proposed using erosion indexes to predict cavitation erosion using CFD, and have applied these indexes to propellers for efficiency verification [3][4]. However, there are limited studies using erosion indexes for internal flows such as control valves, and it is unclear which indexes are the most effective.

Nomenclature

C_v	:flow coefficient
P	:pressure
Q	:volume flow rate
\dot{m}^+, \dot{m}^-	:mass transfer rates
α	:void fraction
σ	:cavitation coefficient
ρ	:mixture density

Subscripts

D	:downstream
U	:upstream
l	:liquid phase
v	:vapor phase

The purpose of this study is to predict cavitation erosion occurrences in control valves by performing CFD modelling of unsteady cavitation flows. We applied the currently proposed 4-type erosion index to predict erosion

2 CFD analysis of the angle valve

2.1 CFD model

The contoured type angle valve to be analyzed is as shown in Fig.1. A 1.5" valve with a flow-to-open direction was used in order to compare the experimental results with those of Yuzawa et al. With diameter D , the upstream and downstream pipe lengths were modelled at $2D$ and $6D$, respectively. CFD analysis was conducted with valve openings of 90% and 100%.

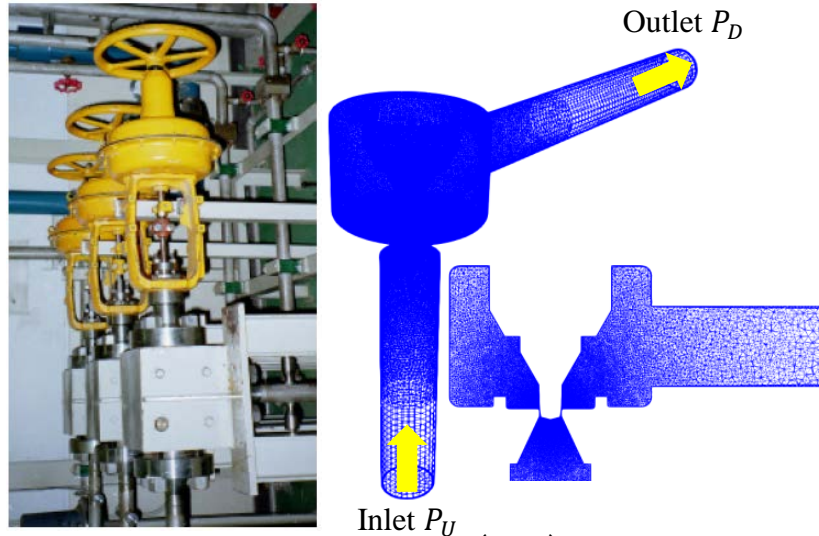


Fig.1 Angle valve (1.5 ")

2.2 CFD conditions

The conditions of the CFD analysis are shown in Table.1. The solver used Advance/Frontflow/Red Ver5.4, a general-purpose fluid analysis code. The cavitation model used the homogeneous flow model proposed by Ikohagi et al. [5] with the following equations:

$$\dot{m} = \begin{cases} \dot{m}^+ & \text{if } P < P_v^* \\ \dot{m}^- & \text{else} \end{cases} \quad (1)$$

$$\dot{m}^+ = C_e A \alpha (1 - \alpha) \left(\frac{\rho_l}{\rho_v} \right) \frac{P_v^* - P}{\sqrt{2\pi R T_s}}, \quad (2)$$

$$\dot{m}^- = C_c A \alpha (1 - \alpha) \frac{P_v^* - P}{\sqrt{2\pi R T_s}}, \quad (3)$$

$$A = C_a \alpha (1 - \alpha) \quad (4)$$

where T_s is the saturation temperature and $C_1^* = C_e C_a$ and $C_2^* = C_c C_a$ are the empirical model constants. In the contoured control valve, the separation generated at the point of constriction causes a wide range of 3D vortices and swirling flows [6]. Since this is an unsteady flow pattern, it is difficult to express accurately in Reynolds Averaged Navier-Stokes (RANS). We initially calculated the vortex appearance with a larger than mesh resolution in large-eddy simulation (LES) due to the close relationship between cavitation behavior and vortices.

The static pressure boundary was given to inlet and outlet, and wall boundaries are given as Spalding-law. Cavitation generation and collapse were expected to occur repeatedly in the area of vena contracta (point of maximum constriction) and hence the mesh resolution was defined around the plug high.

Table.1 CFD analysis settings

Software		Advance/FrontFlow/Red Ver5.4
Turbulent model		Large Eddy Simulation (LES)
Fluid		Water (25°C, compressible)
Number of cells	Travel 100 %	6,723,867
	Travel 90 %	7,899,316
Advection term discrete scheme	Momentum	2 nd order upwind
	Energy	1 st order upwind
Low of the wall		Spalding's low
Simulation time step Δt [s]		$2 \times 10^{-6} \sim 1 \times 10^{-5}$
Number of parallels		288

2.3 Simulation results

Validation of the cavitation analysis was done using CFD with the conditions listed in Table.1 and the CFD analysis and experimental conditions are given in Table.2. These are the same conditions in which Yuzawa et al visualized the occurrence of cavitation. Verification was done by comparing the CFD results with those of the experimental results. Cavitation coefficient σ is used to represent the extent of cavitation and is defined as

$$\sigma = \frac{P_U - P_V}{P_U - P_D} \quad (5)$$

The analytical and experimental C_v are given in Table.3 and Fig.2, and the cavitation visualization results are shown in Fig.3. The range of void fraction contour is visualized with a value of 0.05. A value comparison between the CFD analysis and the experiment shows 2% error of C_v converted from the volume flow and a comparable occurrence of cavitation.

Table.2 Experimental and CFD conditions

Cavitation number σ	P_U [kPa (abs)]	P_D [kPa (abs)]	Travel [%]
1.13	1100	128.7	100

Table.3 CFD analysis results

Flow rate Q [m ³ /h]	C_v
2.889	1.07

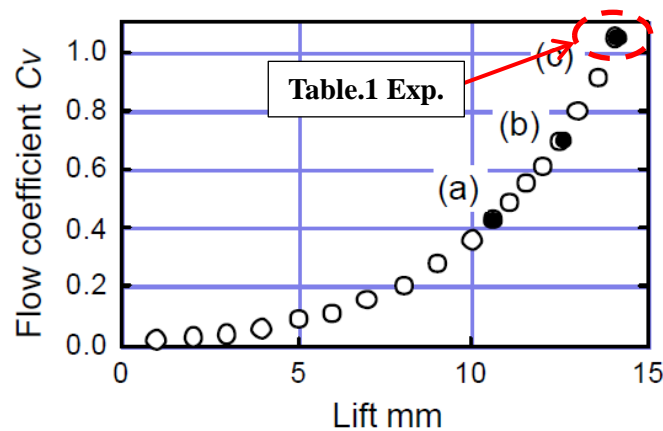


Fig.2 C_v by experiment at $P_U=1$ [MPa][2]

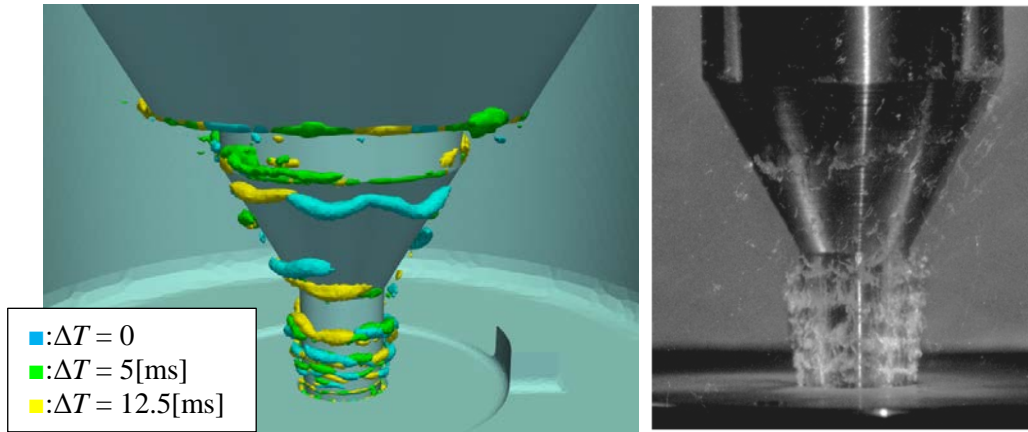


Fig.3 Cavitation features at $P_U=1$ [MPa]

3 Simulation of erosion indexes

3.1 Erosion indexes

Erosion indexes are physical models that use bubble and pressure values to predict erosion risk. These models compute the magnitude of cavitation erosion as a modulus of change of void fraction and pressure on surfaces. The following erosion indexes are proposed by Nohmi et al [4][7].

$$\text{Index1} : \frac{1}{T_c} \int_0^{T_c} \alpha \cdot \max \left[\frac{\partial P}{\partial t}, 0 \right] dt \quad (6)$$

$$\text{Index2} : \frac{1}{T_c} \int_0^{T_c} \alpha \cdot \max [P - P_v, 0] dt \quad (7)$$

$$\text{Index3} : \frac{1}{T_c} \int_0^{T_c} \max \left[-\frac{\partial \alpha}{\partial t}, 0 \right] dt \quad (8)$$

$$\text{Index4} : \frac{1}{T_c} \int_0^{T_c} \max [P - P_v, 0] \cdot \max \left[-\frac{\partial \alpha}{\partial t}, 0 \right] dt \quad (9)$$

Where T_c is the period of the cavitation.

3.2 Comparison of erosion indexes and experimental results

The erosion indexes from section 3.1 were compared with the experimental results to examine the superiority of each one. Specifying trim material of SUS316 and a time period of 30 hours, the CFD analysis and experimental test parameters are given in Table.4 and the results shown in Figs.4 and 5.

Erosion mainly occurs at the seat, taper, and end of taper surfaces (See Fig.7), however this was not reflected in the results where different points of cavitation erosion occurred. In the experimental result of case 1, the plug sheet surface displays the highest erosion while case 2 displays erosion at the taper surface of the plug.

The erosion index results at Index 3 for case 1 show a higher cavitation erosion value at the plug tip than at the seat surface which contradicts the results of the experiment.

The other indexes did not show much difference, and effectively identified the risk of erosion location.

Table.4 Erosion test conditions and flow rate results

	Cavitation number σ	P_U [MPa (abs)]	P_D [MPa (abs)]	Travel [%]	Flow rate Q [m ³ /h]	
					Simulation	Experiment
Case 1	1.058	20	1	90	8.53	8.75
Case 2	1.041	20	0.8		8.63	8.82

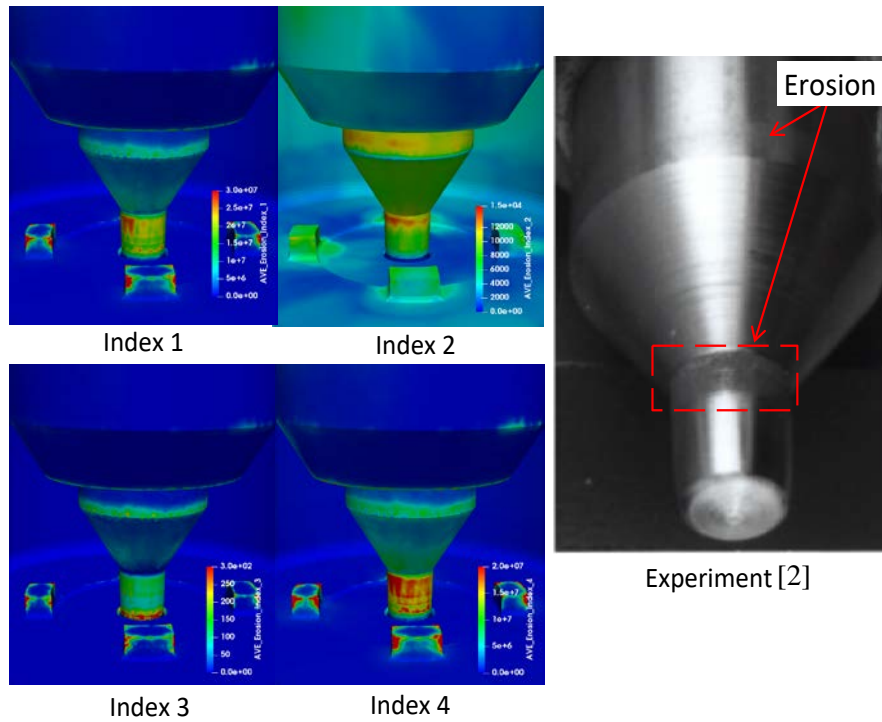


Fig.4 Erosion test results (Case 1)

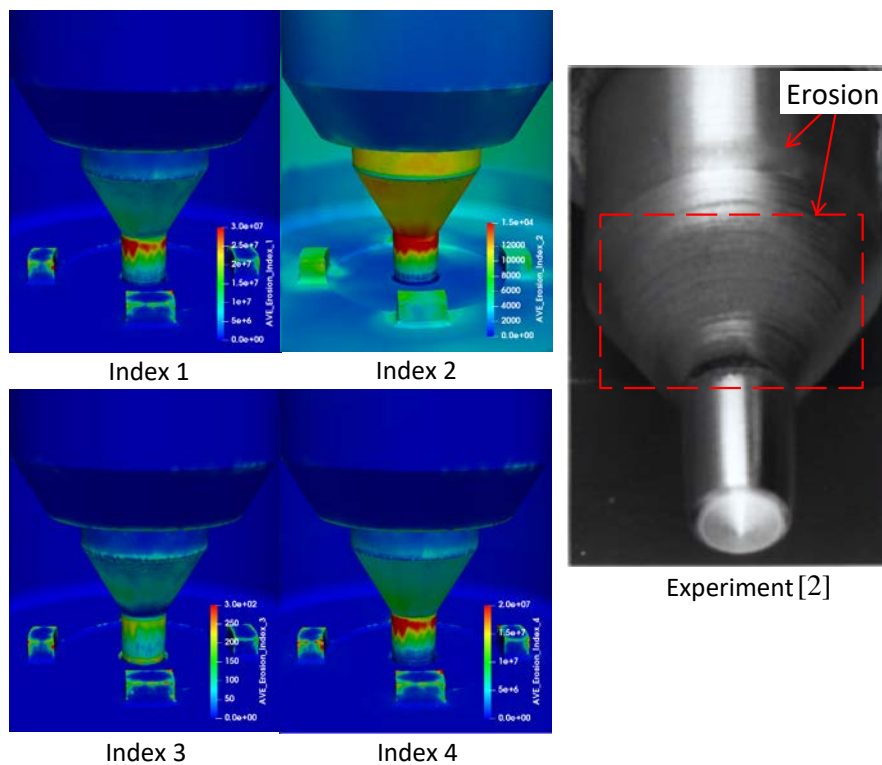


Fig.5 Erosion test results (Case 2)

4 Discussion of erosion indexes

4.1 Erosion by cavitation flow

To explain the relationship between the CFD results and cavitation erosion, Fig 6 depicts the void fraction contour when the simulation time step is passed by ΔT and indicates that cavitation erosion occurs at vena contracta. In case 1, cavitation bubble flows are observed from upstream to downstream along the surface of the plug and collapse. These bubbles, as shown in Fig.3, have an annular shape and are considered to be

cloud cavitation generated by vortices detached from the plug and seat ring boundary layer.

On the other hand, the plug characteristic portion is covered by a layer of cavitation which is allegedly due to developed sheet cavitation. Sheet cavitation composes a relatively stable vapor phase in front of the plug, and then separates it downstream. A separated cavitation becomes a crowd cavitation and collapses the tapered surface. In the context of this research, cloud cavitation greatly affects erosion and the collapse position of cavitation by the CFD analysis agrees with the experimental erosion results. The theoretical relationship between cavitation and erosion generated on the plug surface was confirmed by the CFD modelling of cavitation flows performed in this research.

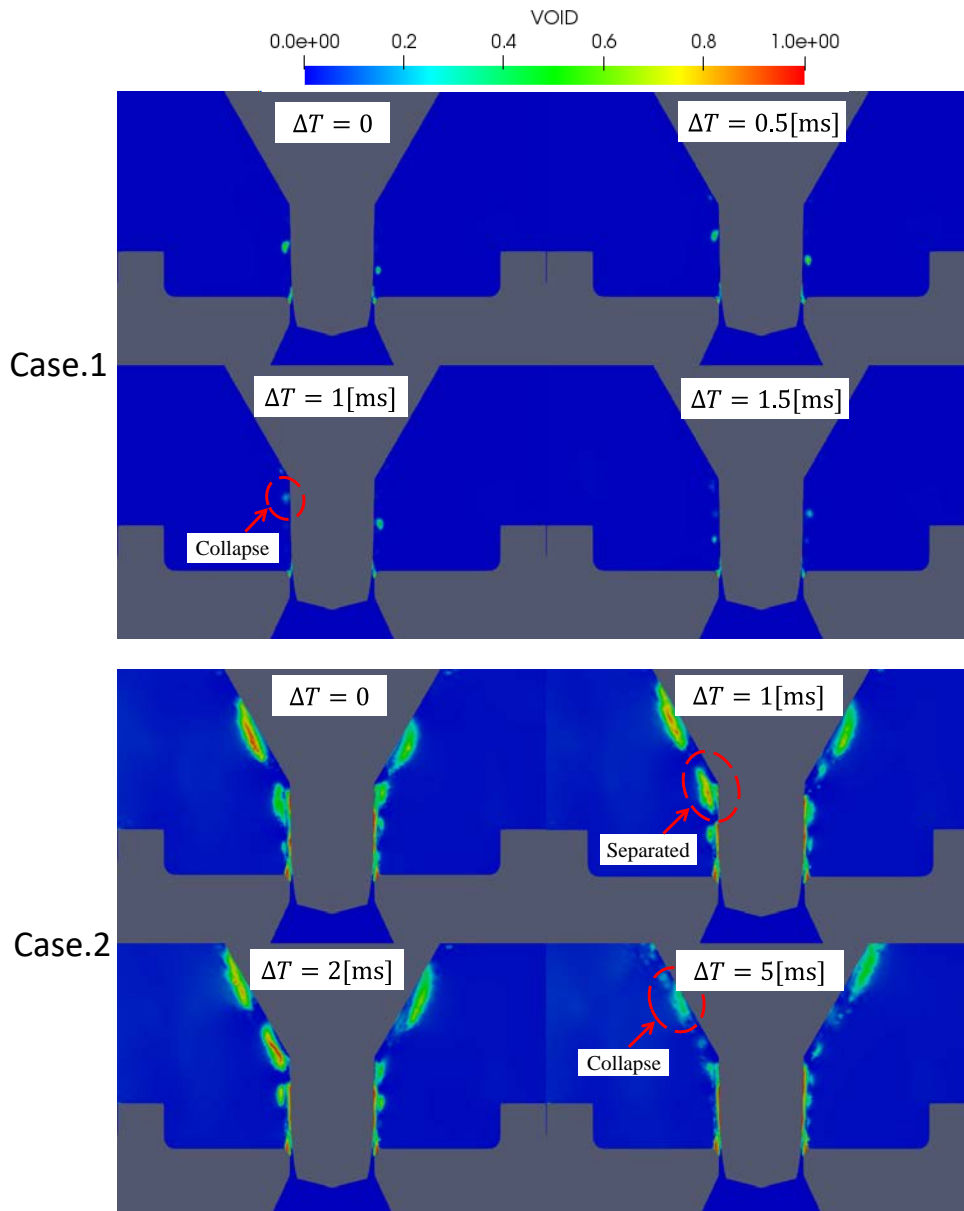


Fig.6 Void fraction contour on plug surface

4.2 Prediction of erosion using erosion indexes

As stated in section 3.2, the experimental results from cases 1 and 2 show that the erosion position is dictated by and changes according to the pressure conditions. The evaluation of the erosion indexes is therefore conducted on the plug surface within a specific area as shown in Fig.7. The evaluation range, calculated from the results in Chapter 3, is given in Table.5 and subsequently divides the sum of the erosion indexes by area.

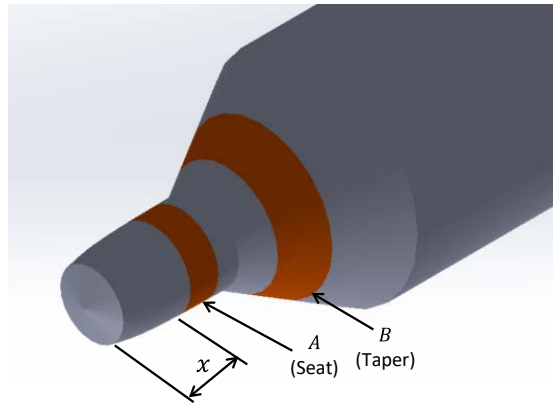


Fig.7 Evaluation surface of erosion index

Table.5 Evaluation position of erosion index

Evaluation surface	A (Seat) [mm]	B (Taper) [mm]
Displacement x[mm]	144±2	155±2.5

The erosion index results are shown in Fig 8. Although the values in the vicinity of the plug seat are lower in case 1 compared to case 2, Index 2 hardly changes. However, a significant difference can be observed between Index 1 and Index 4 and for taper surfaces, all erosion indexes are higher in case 2. These results are valid from the result of cavitation erosion. Simulations with Index 1 and Index 4 appear to agree strongly with experimental results, however, when comparing to the index values of the seat where erosion does not occur, the taper index value tends to be lower. Therefore, further research is needed in order to use cavitation indexes as thresholds.

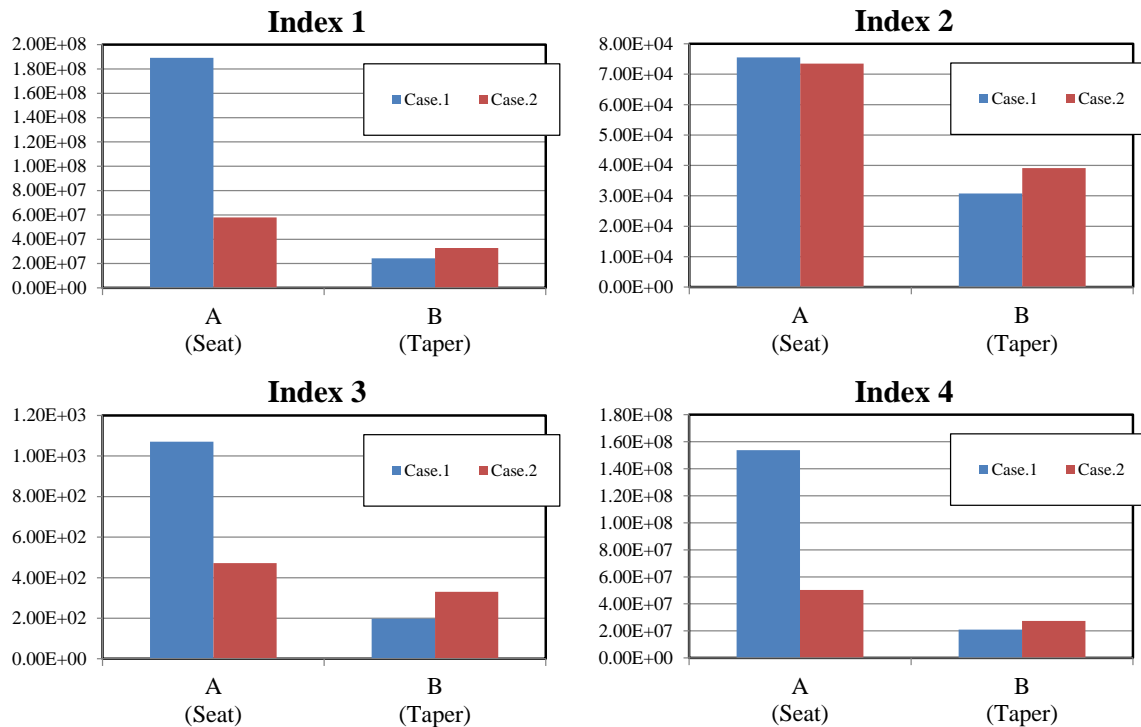


Fig.8 Value of erosion indexes

5 Conclusion

In this study, in order to predict the erosion location in an angle type control valve, the effectiveness of the proposed four erosion index from CFD and experimental results was evaluated and produced the following results:

1. The erosion indexes 1, 2 and 4 were effective in the prediction of the location of erosion
2. Void ratio change was analyzed and clarified the generation mechanism of erosion on the plug surface
3. It proved difficult to judge the occurrence of erosion from the value of each erosion index

References

- [1] G.Kuiper (2001) NEW DEVELOPMENTS AROUND SHEET AND TIP VORTEX CAVITATION ON SHIPS'PROPELLERS, *Fourth International Symposium on Cavitation (CAV2001)*, CA USA.
- [2] S.Yuzawa (2003) Cavitation and Erosion in Control Valves by Pressure Reduction and Flow Regulation of High Pressure Liquid (in Japanese), *Doctoral Dissertation of Waseda University*.
- [3] Onur Usta, Batuhan Aktas et al.(2017) A study on the numerical prediction of cavitation erosion for propellers, *Fifth International Symposium on Marine Propulsion*, Finland.
- [4] N.Hasuike, S.Yamasaki et al.(2011) Numerical Study on Cavitation Erosion Risk of Marine Propellers Operating in Wake Flow, *Journal of the JIME*, Vol. 46, No.3, pp 79-87
- [5] Y.Saito, T.Ikohagi et al.(2003) NUMERICAL ANALYSIS OF UNSTEADY VAPOROUS CAVITATING FLOW AROUND A HYDROFOIL, *Fifth International Symposium on Cavitation (CAV2003)*, Osaka, Japan.
- [6] F.Inoue, E.Outa et al.(1991) An Experimental Study on Control Valve Cavitation (2nd Report, String Bubble Cavitation in Contoured-plug Valve), *Transactions of the Japan Society of Mechanical Engineers*, Series B, Vol. 57, No 544
- [7] M.Nohmi, T.Ikohagi et al.(2008) Numerical Prediction Method of Cavitation Erosion, *ASME Fluids Engineering Division Summer Conference*, FL, USA.